/N -2 4

/

Internal Passage Heat Transfer Prediction Using Multiblock Grids and a k-ω Turbulence Model

David L. Rigby
NYMA, Inc.
Brook Park, Ohio

Ali A. Ameri
AYT Corporation
Brook Park, Ohio

Erlendur Steinthorsson
Institute for Computational Mechanics in Propulsion
Cleveland, Ohio

October 1996

National Aeronautics and
Space Administration

INTERNAL PASSAGE HEAT TRANSFER PREDICTION USING
MULTIBLOCK GRIDS AND A k-ω TURBULENCE MODEL

David L. Rigby*
NYMA, INC.

A. A. Ameri*
AYT Corporation, Brook Park, Ohio

E. Steinthorsson
Institute for Computation of Mechanics of Propulsion (ICOMP)
NASA Lewis Research Center

ABSTRACT

Numerical simulations of the three-dimensional flow and heat transfer in a rectangular duct with a 180° bend were performed. Results are presented for Reynolds numbers of 17,000 and 37,000 and for aspect ratios of 0.5 and 1.0. A k-ω turbulence model with no reference to distance to a wall is used. Direct comparison between single block and multiblock grid calculations are made. Heat transfer and velocity distributions are compared to available literature with good agreement. The multi-block grid system is seen to produce more accurate results compared to a single-block grid with the same number of cells.

NOMENCLATURE

A	Flow area
C_f	Friction coefficient, $2\tau_w/\rho V^2$
D	Hydraulic diameter=4 A/P or turbulent dissipation
H	Channel height
k	Thermal conductivity or turbulent kinetic energy
l	Turbulent length scale, $\sqrt{k}/\omega$
L	Channel length
$\dot{m}$	Mass flow rate
Nu	Nusselt number, hD/k
P	Wetted Perimeter of duct or production of k
Pr	Prandtl number
Re	Reynolds number, VD/ν
S	Distance along the blade surface
T	Temperature
V	Characteristic velocity, $\dot{m}/(\rho A)$
y+	Dimensionless distance from the wall, $\frac{\eta}{D}Re\sqrt{\frac{C_f}{2}}$
ε	Turbulence dissipation rate
η	Distance normal to wall
γ	Specific heat ratio
μ	Viscosity
ρ	Density
ν	Kinematic viscosity
ω	Specific dissipation of turbulence, $\frac{\varepsilon}{k}$
τ_w	Wall shear stress

Subscripts

cent	Centerline value
in	Condition at inlet
prof	profile
t	Total condition or turbulence quantity
w	Wall value
0	Fully developed value

INTRODUCTION

Future generations of ultra high bypass-ratio jet engines will require far higher pressure ratios and operating temperatures than those of current engines. For the foreseeable future, engine materials will not be able to withstand the high temperatures without some form of cooling. In particular the turbine blades, which are under high thermal as well as mechanical loads, must be cooled (Taylor, 1980, Suo, 1978 and Snyder and Roelke, 1990). Cooling of turbine blades is achieved by bleeding air from the compressor stage of the engine through complicated internal passages in the turbine blades (internal cooling, including jet-impingement cooling) and by bleeding small amounts of air into the boundary layer of the external flow through small discrete holes on the surface of the blade (film cooling and transpiration cooling). The cooling must be done using a minimum amount of air or any increases in efficiency

---

gained through higher operating temperature will be lost due to added load on the compressor stage.

The designs of turbine cooling schemes have traditionally been based on extensive empirical data bases, quasi-one-dimensional computational fluid dynamics (CFD) analysis, and trial and error. With improved capabilities of CFD, these traditional methods can be augmented by full three-dimensional simulations of the coolant flow to predict in detail the heat transfer and metal temperatures. Several aspects of turbine coolant flows make such application of CFD difficult, thus a highly effective CFD methodology must be used. First, high resolution of the flow field is required to attain the needed accuracy for heat transfer predictions, making highly efficient flow solvers essential for such computations. Second, the geometries of the flow passages are complicated but must be modeled accurately in order to capture all important details of the flow. This makes grid generation and grid quality important issues. Finally, since coolant flows are turbulent and separated the effects of turbulence must be modeled with a low Reynolds number turbulence model to accurately predict details of heat transfer.

The overall objective of our ongoing research is to develop a CFD methodology that can be used effectively to design and evaluate turbine cooling schemes. In this study, we focus on two aspects of CFD for turbine cooling, namely grid structures for coolant passage geometries and turbulence modeling for coolant flows. Grid generation for complicated geometries such as coolant passages, is currently an active area of research. In general, grid systems for complicated geometries are classified as block-structured, unstructured or hybrid. Of those, unstructured grids offer the greatest flexibility for modeling of complex geometries and the generation of unstructured grids is largely automatic. In contrast, fully continuous block-structured grids, where all grid lines are at least C^1 continuous across block faces (here referred to as multi-block grids), are more difficult to generate but are the most suitable for simulations of viscous flows. In addition, flow solvers for structured grids typically require less memory than those for unstructured grids, and can take full advantage of various convergence acceleration schemes (e.g. multigrid) and fast solvers for implicit discretizations (e.g., line Gauss-Seidel, approximate LU and ADI schemes). In this study, we use semi-automatically generated multiblock grids (i.e., shape of blocks is automatically determined but grid-topology or block-structure needs to be specified beforehand).

Turbulence models used in simulations of internal flows in complicated geometries must be able to model flows involving separation and adverse pressure gradients. One such model is the k-ω model of Wilcox(1994a and 1994b). This model has several desirable features. One important feature is that it does not require distance to a nearest wall as a parameter. Second, the low Reynolds number version of the model can be used to
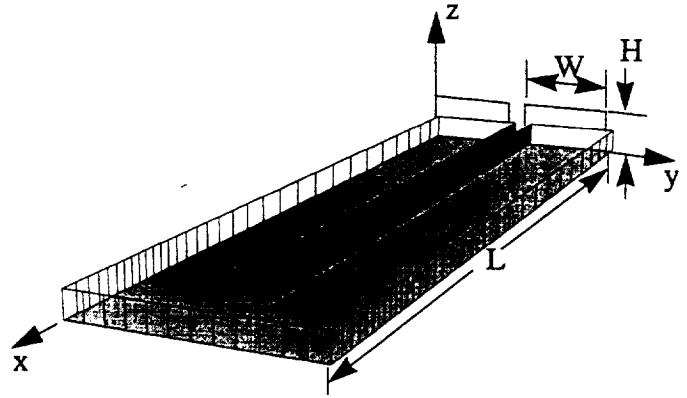

Figure 1. Geometry

model transition (Wilcox, 1994b). Finally, as both k and ω are well behaved numerically, stiffness associated with low-Reynolds number k-ε turbulence models is eliminated. In addition recent work by Chima (1996) show the model to be useful for predicting heat transfer over turbine blades.

To test the multiblock grid system and the k-ω model for internal flows, flow and heat transfer in rectangular ducts with 180 degree turn (see Fig. 1) were simulated. The simulations were performed using both a traditional single block grid system and a multi-block grid system. Results for ducts with aspect ratio of 1.0 and 0.5 are presented. In this paper, the computed results are compared with experimental data reported by Arts, et al. (1992) for those same geometries. The flow conditions chosen for the simulations are the same as those used in the experiments.

Several workers have investigated the flow and heat transfer in 180° turns in the past, including Prakash and Zerkle (1992) Tekriwal (1994) and Besserman and Tanrikut (1991). Effects of factors such as rotation, inlet and exit boundary conditions as well as wall heat transfer boundary conditions have been investigated. Such effects were investigated using a high Reynolds number k-ε model with wall functions and/or low Reynolds number turbulence models. To limit the scope of the present study, such aspects were not investigated. Rather, an attempt was made to account accurately for the conditions used in the experiment by Arts et. al. and to focus on evaluation of the low Reynolds number $k-\omega$ model for heat transfer prediction.

The remainder of this paper is organized as follows: After this introduction, the test problem is described. Then the numerical method used in the simulations is outlined and boundary conditions used to obtain proper entrance flow conditions are described. Subsequently, the grid systems used for the simulations are discussed, and the k-ω turbulence model and its implementation is described. Finally, the results of the

computations are shown and compared to the experimental data. The paper ends with a summary and conclusions.

DESCRIPTION OF PROBLEM

The geometry of the 180 degree turn is shown in Fig 1. The inlet and exit channels have the same cross sectional shape. Aspect ratio of 1.0 (H=W) and 0.5 (H=W/2) are considered in the present work. The overall length of the channel is 8W. The divider has thickness of W/5 and extends to within one width of the end wall. The divider has a semi-circular end. At the inlet, fully developed velocity and temperature profiles are imposed. Symmetry is enforced at half of the channel height. The temperature of all walls are specified to be at $1.1T_{t, in}$, where $T_{t, in}$ is the centerline inlet total temperature. Reynolds number based on hydraulic diameter of 17,000 and 37,000 are considered.

COMPUTATIONAL METHOD

The simulations performed in this study were done using a computer code called TRAF3D.MB (Steinthorsson et al. 1993). This code is a general purpose flow solver, designed for simulations of flows in complicated geometries. The code is based on the TRAF3D code, an efficient computer code designed for simulations of flows in turbine cascades (Arnone et al. 1991). The TRAF3D.MB code employs the full compressible Navier-Stokes equations. It uses a multi-stage Runge-Kutta scheme to march in pseudo time. The code utilizes multi-grid and implicit residual smoothing to accelerate convergence to steady state. Convective and diffusive fluxes are computed using central differencing. Artificial dissipation is added to prevent odd-even decoupling. The discretization is formally second order accurate. To handle complex geometries, the code uses contiguous multiblock grid systems but has the added capability of handling grids with non-contiguous grid lines across branch cuts. For contiguous systems, all internal boundaries are conservative. The TRAF3D.MB code was described in detail by Steinthorsson et al. (1993). Some aspects of the formulation used in the code are the same as those described by Arnone et al. (1991). For the present computations the code was fitted with the low Reynolds number k-ω model of Wilcox (Chima, 1996).

Turbulence Model

When using a multiblock approach it is advantageous to use a set of equations describing the turbulence that does not require the computation of the dimensionless distance to the wall y^+. The boundaries between adjacent blocks should be free to cut across boundary layers and regions of high shear. Having to carry information on solid walls and dealing with corners requires communication of much information that is quite cumbersome and time consuming both in terms of programming and CPU time.

The k-ω turbulence model developed by Wilcox

(1994a,1994b) satisfy our requirements. Subsequent modifications by Menter (1993) improved the robustness of the model. Recently, Chima (1996) incorporated some of the latter modifications to the turbulence model and presented some applications of this model in the context of a Navier-Stokes solver. In fact it is the three-dimensional variation to the formulation adapted by Chima that has been utilized in this paper. Chima has shown the model to possess very good convergence properties. He also showed that the model performs well in predicting the rate of heat transfer from a simulated flat plate and turbine blades under various conditions. Below we present the equations describing the turbulence in tensor notation.

$$(\rho s_i)_{,t} + (\rho s_i u_j + q_{ij})_{,j} = \frac{1}{\rho}(P - D) \tag{1}$$

$$q_{i,j} = -\left(\mu + \frac{\mu_t}{\sigma}\right)s_{i,j} \quad j=1,3 \tag{2}$$

where s_1=k and s_2=ω also $\mu_t = \alpha^* \dfrac{\rho k}{\omega}$

The source terms, P, of equation (1) are defined as

$$\frac{P}{\rho} = \begin{bmatrix} \dfrac{Re^{-1}}{\rho}\mu_t\Omega^2 - \dfrac{2k}{3}(\nabla \bullet V) \\[2mm] \alpha\left[\alpha^*\Omega^2 - \dfrac{2}{3}\omega(\nabla \bullet V)\right] \end{bmatrix} \tag{3}$$

where Ω is the vorticity. The destruction terms, D, are given by

$$\frac{D}{\rho} = \begin{bmatrix} \beta^*\omega k \\[1mm] \beta\omega^2 \end{bmatrix} \tag{4}$$

The coefficients appearing in the model are

σ=0.5, β=3/40, β^*=0.09F_β, α=(5/9)(F_α/F_μ), and α^*=F_μ, where

$$F_\beta = \frac{\dfrac{5}{18} + \left(\dfrac{Re_T}{R_\beta}\right)^4}{1 + \left(\dfrac{Re_T}{R_\beta}\right)^4} \tag{5}$$

$$F_\alpha = \frac{\alpha_0 + \left(\dfrac{Re_T}{R_\omega}\right)}{1 + \left(\dfrac{Re_T}{R_\omega}\right)} \tag{6}$$

$$F_\mu = \frac{\alpha_0 + \left(\frac{Re_T}{R_k}\right)}{1 + \left(\frac{Re_T}{R_k}\right)} \qquad (7)$$

$$Re_T = \frac{\rho k}{\mu \omega} \qquad (8)$$

Above $\alpha_0=0.1$, $\alpha_0^*=0.025$, $R_\beta=8$, $R_\omega=0.27$ and $R_k=6$.

Boundary Conditions

The types of boundary conditions encountered in solving the problem at hand are as follows:

1) Inlet: The inlet boundary condition for subsonic flows is treated by specifying the total inlet temperature and total inlet pressure as well as the inlet angle profiles. The outgoing Riemann invariant is extrapolated to the inlet from within. The total temperature and pressure profiles are chosen to produce specified velocity and temperature profiles. In the present work, velocity and temperature profiles which are reasonably valid for fully developed circular pipe flow are mapped to the present rectangular shape. These profiles are obtained as follows:

For a flat plate the law of the wall profiles are (Kays and Crawford, 1980)

$$u_f^+\left(y^+\right) = \begin{bmatrix} y^+ & y^+ < 10.88 \\ 2.5\ln\left(y^+\right) + 5.5 & y^+ \ge 10.88 \end{bmatrix} \qquad (9)$$

$$T_f^+\left(y^+\right) = \begin{bmatrix} Pr\,y^+ & y^+ < 13.2 \\ 2.195\ln\left(y^+\right) + 13.2Pr - (5.66) & y^+ \ge 13.2 \end{bmatrix} \qquad (10)$$

Now, to make these valid for a circular pipe, let

$$y_p^+ = \left(\frac{1.5\left(1 + \frac{r}{R}\right)}{1 + 2\left(\frac{r}{R}\right)^2}\right) y^+ \qquad (11)$$

as suggested by Reichardt (ibid). Using y_p^+ in Eqs. (9-10) produces zero slope at the centerline while near the wall the profile is relatively unaffected. The profiles are then input to the code normalized by the centerline values so that

$$u_{prof} = \frac{u_f^+\left(y_p^+\right)}{u_f^+\left(y_{p,cent}^+\right)} \qquad (12)$$

$$T_{prof} = \frac{T_f^+\left(y_p^+\right)}{T_f^+\left(y_{p,cent}^+\right)} \qquad (13)$$

Since the flow is at low Mach number the total temperature profile is set to T_{prof} and the total pressure profile is defined by

$$p_{t,prof} = \left(1 + \frac{(\gamma-1)}{2}(M_c u_{prof})^2\right)^{\frac{\gamma}{(\gamma-1)}} \qquad (14)$$

where M_c is a specified centerline Mach number.

The turbulent viscosity profile is set to (Kays and Crawford, 1980)

$$\mu_t = \frac{0.4y^+}{6}\left(1 + \frac{r}{R}\right)\left(1 + \left(\frac{r}{R}\right)^2\right) \qquad (15)$$

and the length scale to (Schlichting, 1979)

$$\frac{l}{R} = 0.14 - 0.08\left(\frac{r}{R}\right)^2 - 0.06\left(\frac{r}{R}\right)^4 \qquad (16)$$

Inlet profiles of k and ω are set based on μ_t and l.

2) Exit: At the exit boundary, for subsonic flow, the pressure is specified while all other conditions are extrapolated from within.

3) Walls: At walls, the normal pressure gradient is set to zero, the temperature is specified, and the no-slip condition is enforced. The density and total energy are computed from the pressure and the temperature. The boundary conditions for the turbulence quantities are k=0 and

$$\omega = S_R \frac{\partial u}{\partial y}\bigg|_{wall} \qquad (17)$$

where

$$S_R = \begin{bmatrix} \left(\frac{50}{K_R}\right)^2, & K_R < 25 \\ \frac{100}{K_R}, & K_R \ge 25 \end{bmatrix} \qquad (18)$$

and K_R is the equivalent sand grain roughness height in turbulent wall units. $K_R=5$ was used, corresponding to a hydraulically smooth surface.
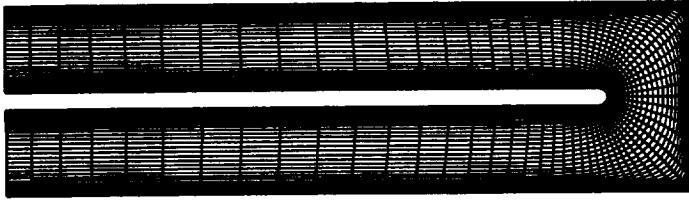
An upper limit is imposed on the value of ω at the wall using the following boundary condition suggested by Menter(1993) and found effective by Chima(1996),

$$\omega_{max} = \frac{10\,6}{Re\beta}\frac{\nu}{\Delta y^2} \qquad (19)$$

COMPUTATIONAL GRID

Two types of grids are used in this study to model the geometry of the duct in Fig. 1. Both grid types are body-fitted

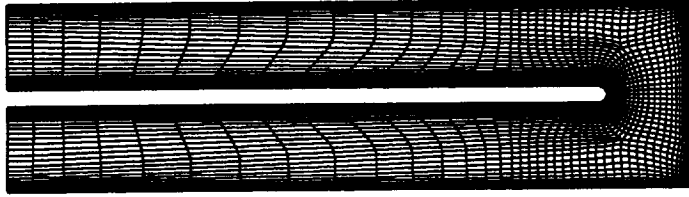a. single block medium grid

b. multiblock grid

Figure 2. Example of grids

Figure 3. Convergence history for single and multi-block

structured (mapped) grids. The first is a traditional single-block grid(Fig. 2a), whereas the second is a multi-block grid(Fig. 2b).

In the single-block grid, shown in Fig. 2a, one family of grid lines follows the main streamwise direction of the flow and thus wraps around the inner wall of the duct. This produces a high quality grid on the inner surface of the duct. However, the use of a single block for the grid forces one to make trade-offs between resolution or grid quality in different regions of the duct. In the single-block grid lines go from the rounded section of the inner side wall to the end wall (on the outer side wall). When sufficient resolution is obtained on the section of the inner wall, the end wall is highly under-resolved. Also, with the single block grid it is difficult to get the needed resolution in the two outer corners without producing an excessively refined grid elsewhere or sacrificing grid quality.

The multiblock grid system, shown in Fig. 2b, is designed to give high-quality grids near all solid surfaces. Thus, the block structure is such that grid lines near the inner wall "wrap around" the wall as in the single block grid, while an H-like grid structure is created along the outer wall. To match the grids near the inner wall and the outer wall, one allows topological singularities in the grid structure, where three, five, or more grid lines intersect. By allowing these topological singularities, much more control over resolution, smoothness and orthogonality is obtained. These singularities lie in regions where the flow is less complicated and where gradients are small. The net results is that the grid in the bend is smooth, nearly orthogonal and has the greatest resolution where it is needed.

The single-block grid systems used here were generated using Gridgen (1995) whereas the multi-block grid was generated using a combination of GridPro/az3000 (1993)and Gridgen.
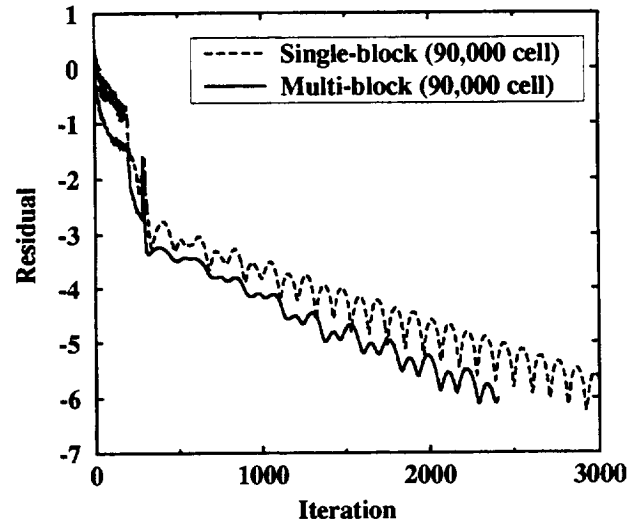
RESULTS AND DISCUSSIONS

Overview of Cases

Numerical solutions of the flow and heat transfer in the duct of Fig. 1 were obtained for a total of four physical cases. Ducts with aspect ratio of 1.0 and 0.5 were calculated at Reynolds numbers of approximately 18000 and 35000. The computed heat transfer and flow-field data are compared with experimental data of Arts, et al.(1992). The results of the computations are shown in Fig. 3-8.

A total of seven numerical runs were performed as outlined in Table 1. First, three single-block runs were done to assess grid requirements at the lower Reynolds number and aspect ratio of 0.5. Then the higher Reynolds number flow was calculated on the single block medium grid. Also, the single block medium grid was stretched in the z-direction to perform calculations at an aspect ratio of 1.0 at the low and high Reynolds numbers. The multi-block grid was used for the 0.5 aspect ratio duct at the lower Reynolds number. For all the lower Reynolds number cases the average y^+ on the bottom wall was about 1.0 with peak values near 3.0.

The resulting Reynolds numbers from the calculations do not exactly match the experiment since the final converged mass flow rate is governed by the fixed pressure ratio. The resulting Reynolds numbers are sufficiently close to the experimental results for direct comparison. This is especially true for the heat transfer results since they are normalized to take into account Reynolds number variation.

5

Grid	Re $x10^3$	$\frac{\Delta z}{W}$	A.R.	Cells $x10^3$
Single Block Coarse	17	.0040	0.5	30
Single Block Medium	17	.0028	0.5	90
Single Block Fine	17	.0020	0.5	270
Multi-block Medium	17	.0028	0.5	90
Single Block Medium	37	.0028	0.5	90
Single Block Medium	17	.0028	1.0	90
Single Block Medium	34	.0028	1.0	90

TABLE 1. Overview of numerical runs.

Figure 3 shows the convergence history for the single-block medium grid and the multi-block grid. It is often expected that multi-block grids will converge slower than single block grids. For the present calculation the convergence was comparable for the two topologies. Apparently any possible harm done by the decoupling in the multi-block grid is offset by improvement due to a better quality grid. It is also conjectured that the multigrid procedure employed in the flow solver provides strong coupling between blocks, minimizing any slow down in convergence which might otherwise result.

Flow Field

Before the computed and experimentally determined heat transfer in the duct is examined, it is informative to examine main features of the flow field in the duct. Fig. 4–6 show the computed flow field in the channel. Figure 4 shows the streamline pattern in the symmetry plane of the duct for the single block fine (Fig. 4a) and the multi-block (Fig. 4b) calculations at Reynolds number of 17,000. The figure reveals the expected recirculation zone in the first outer corner of the duct and the region of separated flow near the inner side wall, at and after the 180 degree turn. The multi-block solution also produces mall recirculation zone at the second outside corner. This is nably due to the superior resolution in the corner regions. .ll that the fine single-block grid has roughly three times as y cells as the multi-block grid but still has poor resolutio. near the outer corners.

In the symmetry plane, the flow separates from the inner side wall at about 60 degrees into the turn. The flow reattaches at about x=5W. Away from the symmetry plane, the size of the recirculation zone is affected by the presence of the secondary flow in the channel. The effect of the secondary flow is to "pinch" the separated region and reduce it's size near the bottom wall.

In Fig. 4 it can be seen how the high-momentum fluid entering the turn from the inflow branch impinges on the end wall. This impingement gives rise to secondary flow as fluid is
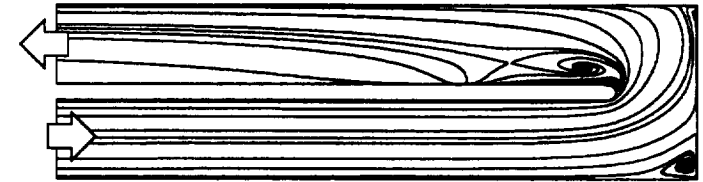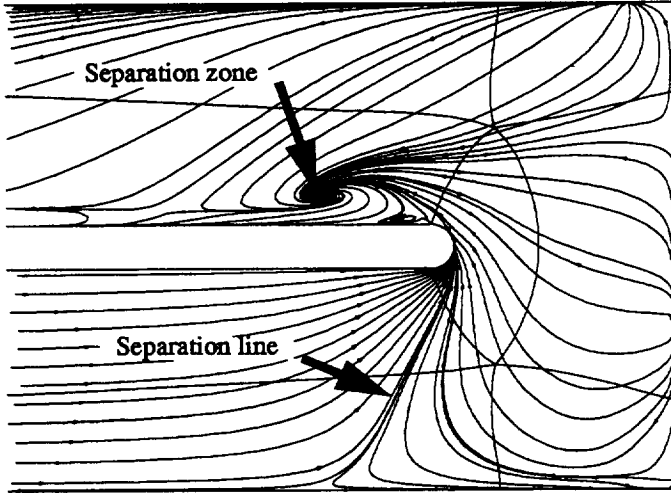

a. single block fine
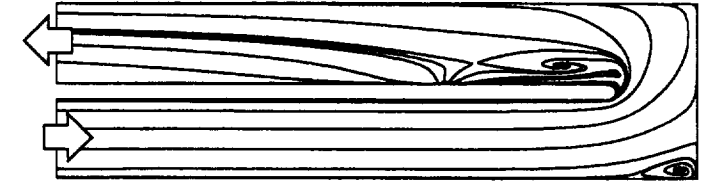
b. multiblock

Figure 4. Symmetry plane streamlines for Reynolds number of 17,000 and aspect ratio of 0.5.

diverted away from the symmetry plane and towards the top and bottom surfaces of the duct (see also Fig. 5a). As the flow turns into the outflow branch of the duct, the high-momentum flow in the symmetry plane again impinges on the outer wall, further strengthening the secondary flow in the duct.

Figure 5 shows simulated oil flow (a) and surface pressure (b) on the bottom wall for the multi-block calculation at a Reynolds number of 17,000 and aspect ratio of 0.5. Overlaid on these plots is the topology of the block structure. Figure 5a shows the presence of the recirculation zone downstream of the inner corner, and also the separation line at the entrance to the turn. Comparison of Fig. 4b and Fig. 5a also reveals that near the bottom surface, the flow direction is vastly different from that in the symmetry plane. Figure 5b shows the normalized pressure on the bottom wall. In Fig. 5b, the separation zone coincides with a low pressure region. This figure also shows that most of the pressure drop in the passage occurs as the flow negotiates the turn.

The secondary flow at x=6.9W in the out-flow branch is shown in Fig. 6. These results are for the aspect ratio of 1.0 and at the higher Reynolds number. The solution for the single block medium grid is shown and has been reflected about the symmetry plane for comparison to the experiment. Also in that figure is a plot of the experimentally determined flow field at the same location. As the figure shows, the secondary flow is reasonably well predicted by the computations. It should be noted that the numerical results for the lower Reynolds number are similar when plotted as in Fig. 6 which indicates that the global topology of the flow is unchanged at this location. Note that only the medium grid was run for this case. A fine single-block or multi-block grid would be expected to compare better quantitatively to the experimental data. These cases were not simulated, however, since the effort was placed on getting heat transfer results which were available for the aspect ratio of 0.5.

6

a.) Simulated oil trace.

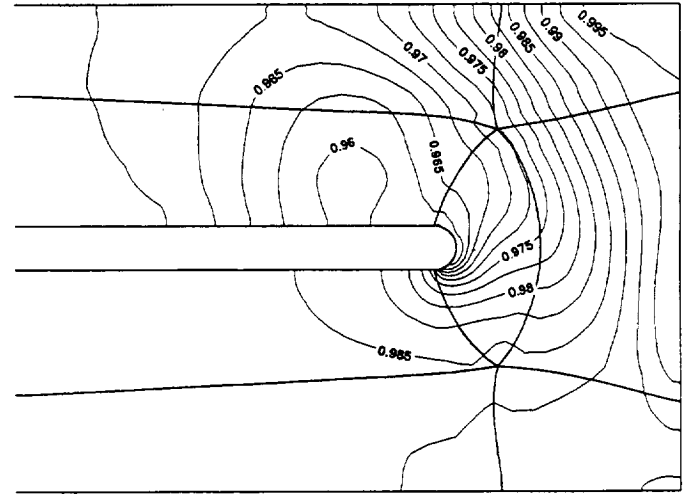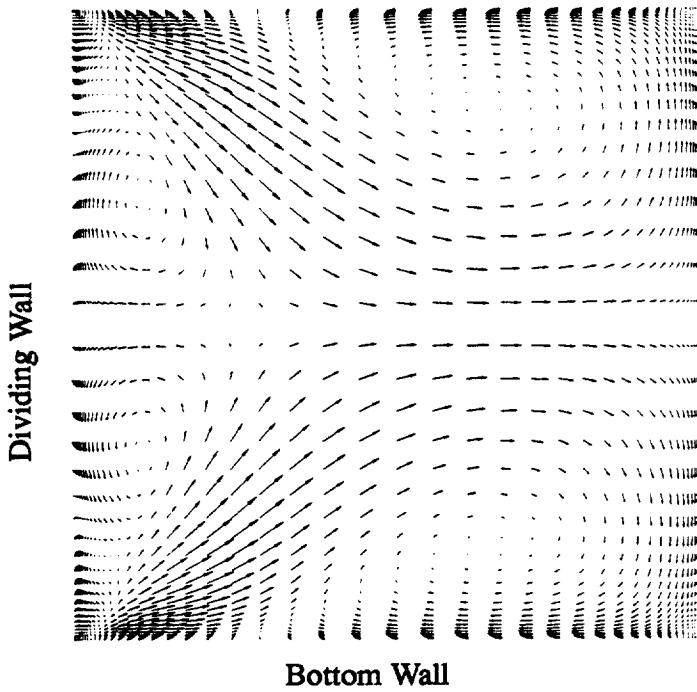b.) Normalized surface pressure.

Figure 5. Bottom wall results for Reynolds number of 17,000 and aspect ratio of 0.5

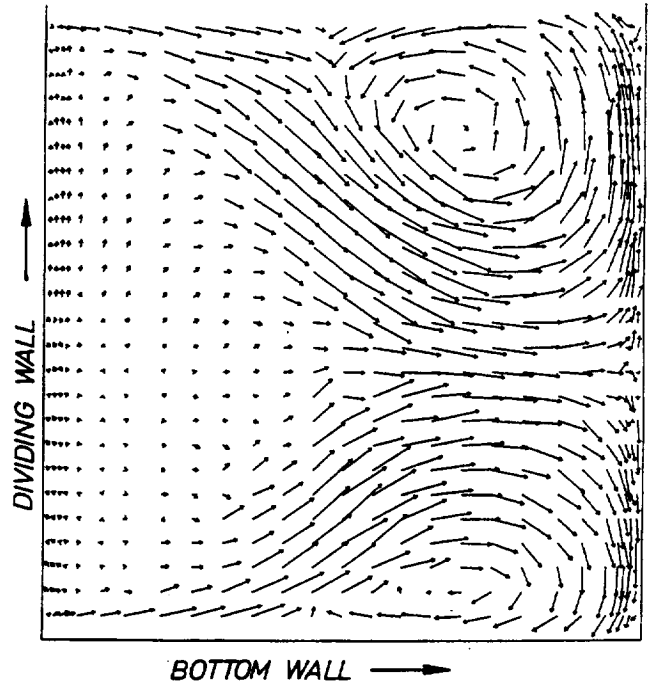a. numerical single block medium grid

b. experiment (Arts et.al. (1992)

Figure 6. Velocity vectors in downstream leg at x=6.9W for Reynolds number of 37,000 and aspect ratio of 0.5.
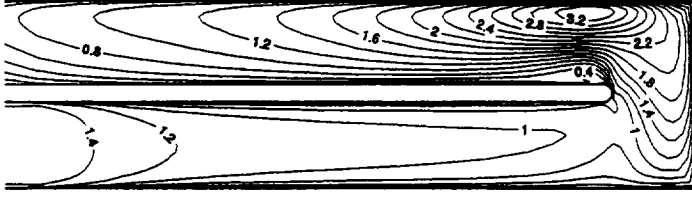
Heat transfer

The heat transfer is presented in the form of the Nusselt number normalized by the value for fully developed turbulent pipe flow. The Nusselt number is defined as

$$Nu = \frac{hD}{k} \qquad (20)$$

where D is the hydraulic diameter and k is the thermal conductivity evaluated at the reference temperature. The reference temperature for the present study is taken to be the average between the inlet and exit centerline temperatures at x=0. The heat transfer coefficient h is defined by

$$h = \frac{q_w}{T_w - T_{ref}} \qquad (21)$$

7

a. single block coarse grid (30,000 cells)

b. single block medium grid (90,000 cells)
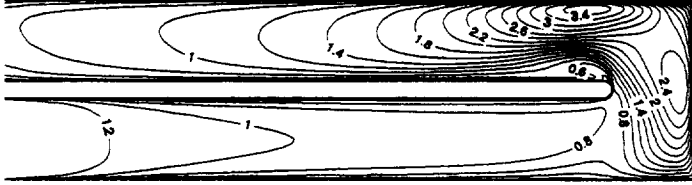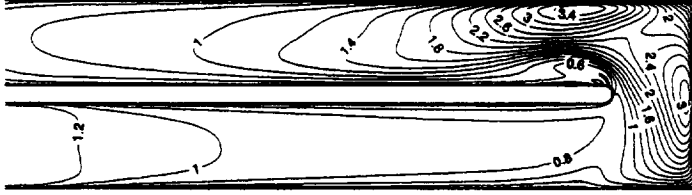

c. single block fine grid (270,000 cells)

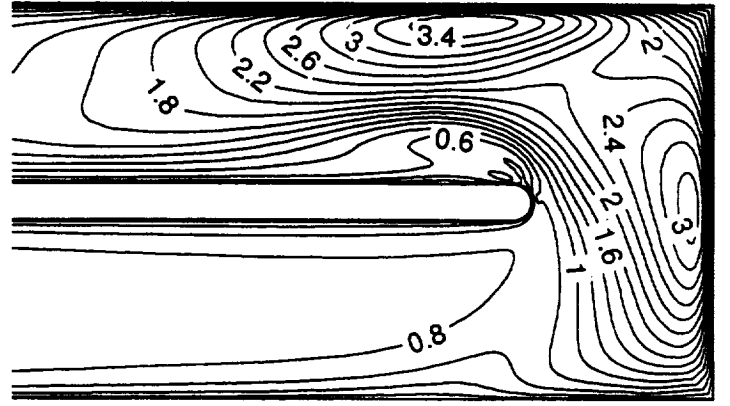Figure 7. Bottom wall heat transfer for aspect ratio 0.5 and Reynolds number of 18,000.

The Nusselt number for fully developed turbulent pipe flow is taken to be

$$Nu_0 = 0.023 Re_D^{0.8} Pr^{0.4} \qquad (22)$$

The computed heat transfer on the bottom wall is shown in Fig. 7 and 8 for the 0.5 aspect ratio and 18000 Reynolds number. Figure 7 shows the heat transfer obtained using three single-block grids, with about 30,000, 90,000 and 270,000 grid points. Figure 8 shows a close-up view of the region around the 180 degree bend for the finest single-block grid, the multi-block grid and the experimental data.

Figure 7 reveals that the results for the medium single-block grid (Fig. 7b) and the finest single-block grid (Fig. 7c) are very similar. Both show two peaks in the heat transfer on the bottom wall, one near the end wall and the other near the outer wall after the second corner. Furthermore, magnitude of the second peak is nearly identical in those two solutions. In contrast, the coarsest solution obtained on the single-block grid (Fig. 7a) does not contain the first of the two peaks in heat transfer. The fact that there still exists some difference between the fine and medium solutions indicates that, even with 270,000 cells, the single-block grid lacks the required resolution in some regions.
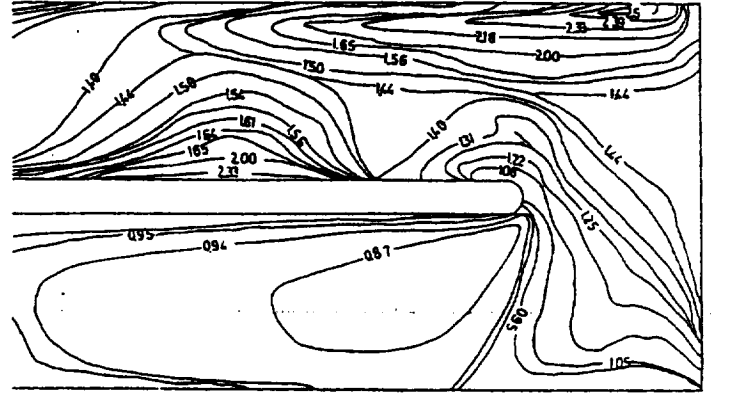
a. single block fine grid (270,000 cells)
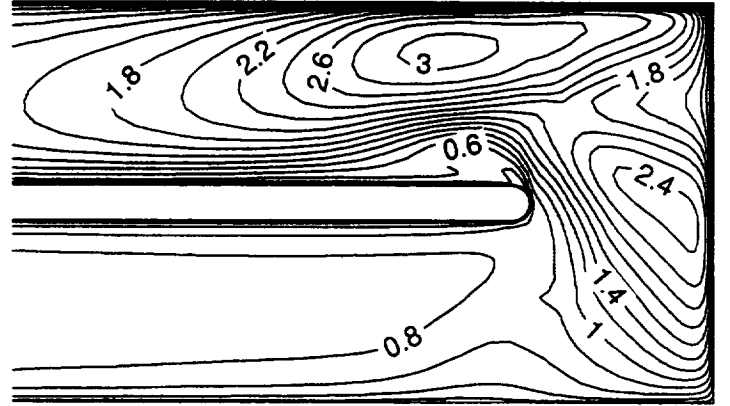
b. multiblock grid (90,000 cells)

c. experiment Arts et. al. (1992)

Figure 8. Bottom wall heat transfer for fine single block (a), multiblock (b), and experiment.

In Fig. 8 it is seen that like the solutions obtained on the medium and fine single-block grids, the solution obtained on the multi-block grid also exhibits the two peaks in heat transfer. However, the peak values of heat transfer predicted using the multi-block grid more closely matches the experimental data.
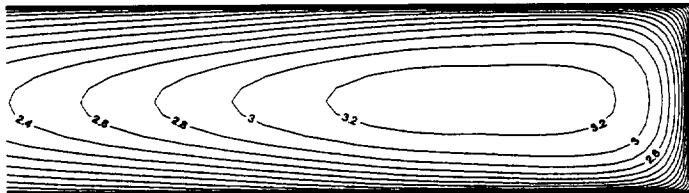
a. single block fine grid (270,000 cells)

b. multiblock grid (90,000 cells)

c. experiment Arts et. al.(1992)
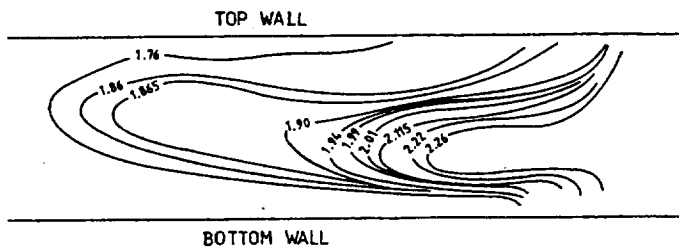
TOP WALL

BOTTOM WALL
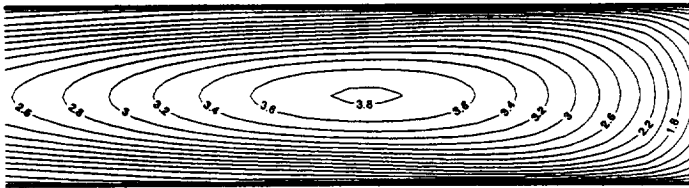
Figure 9. Side wall heat transfer for Reynolds number of 17,000 and aspect ratio of 0.5.

Furthermore, the shape of the contours entering the first corner is better predicted by the multi-block solution.

Although both the single-block and the multi-block grids produce the two peaks in heat transfer, albeit with different degrees of accuracy, neither produces the elevated heat transfer which the experimental data reveals near the inner wall, down-stream of the bend, where the primary separated flow reattaches. Reasons for this deficiency in the computed solution maybe a lack of streamwise resolution at the reattachment point and/or a weakness in the turbulence model. It is also possible that a lack of perfect symmetry in the experimental data exaggerates the heat transfer at this particular location.

Overall, Fig. 7-8 show that multi-block grid systems leads to better results than the traditional single block grid, even for this relatively simple geometry. Also, the k-ω turbulence model appears to perform well, giving the right level of heat transfer although the peak values appear to be over predicted. This over prediction could also be related to the lack of symmetry in the experimental data (see Fig. 6b and Fig. 9c). It should be noted that levels of Nu/Nu_0 greater than three are not uncommon in these types of flows. Boyle(1984) presents results for a very similar geometry showing heat transfer results along the centerline of the channel which go above three times the fully
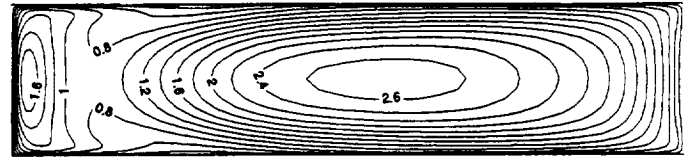

Figure 10. End wall heat transfer for Reynolds number of 17,000 and aspect ratio of 0.5.

developed turbulent pipe flow value, which is consistent with the present results.

Figure 9 shows the heat transfer on the outer wall of the return channel of the duct at Reynolds number of 17,000 and aspect ratio of 0.5. The figure shows the heat transfer obtained on the single-block fine grid, the multi-block grid and it shows the experimental data of Arts et al. (1992). As expected, a peak in the heat transfer is observed a short distance from the corner, where the high-momentum fluid in the center of the duct impinges on the side wall. The location of the peak obtained with the multiblock grid matches the experimental data well, whereas with the single block grid the location of the peak is too far down stream of the corner by nearly half the width of the channel.

The heat transfer on the endwall is shown in Fig. 10. This figure shows the peak value to be at the midspan of the passage where the flow from the first leg impinges on the endwall. Also in Fig. 10 is a line of lower heat transfer near the second corner which corresponds to the separation line associated with the vortex formed in that corner.

CONCLUSIONS

In this study, flow and heat transfer in rectangular ducts with a 180 degree turn has been simulated. The geometry of the ducts represent configurations found in internal coolant passages of turbine blades. The computed heat transfer was compared to the experimental data of Arts et. al. The computed results, show that reasonable accuracy can be obtained for heat transfer in internal coolant passages.

Two sets of numerical solutions were presented. The first was obtained using a single-block grid system. The second was obtained with a multi-block grid system with the same number of cells as the medium single-block grid. Comparison of the two sets of results revealed that the multi-block grid system yielded better results than even the fine single-block grid. The key difference between the grids is the inferior resolution and orthogonality of the single-block grid in the outer corners of the bend. Although the lack of resolution and orthogonality in the single-block grid is confined to a small region in the corners, it causes substantial difference in the computed solutions. This sensitivity demonstrates the need for particular attention to grid quality and resolution even in regions where the solution may not be of interest.

The k-ω turbulence model of Wilcox(1994a,b) was found to do a reasonable job of modeling the effects of turbulence on

the mean flow and heat transfer, without requiring reference to distance to solid surfaces. The model was also found to behave well numerically. The combination of multi-block grids and the k-ω turbulence model appears to be a promising approach to simulating flow and heat transfer in complex turbine coolant passages.

REFERENCES

Arnone, A., Liou, M.-S., and Povinelli, L. A.,1991, "Multigrid Calculation of Three-Dimensional Viscous Cascade Flows," AIAA-91-3238.

Arts, T., Lambert de Rouvroit, M., Rau, G. and Acton, P, 1992, "Aero-Thermal Investigation of the Flow Developing in a 180 Degree Turn Channel," VKI pre-print No 1992-10.

Besserman, D.L. and Tanrikut, S., 1991, "Comparison of Heat Transfer Measurements with Computations for Turbulent Flow Around a 180 Degree Bend", ASME paper 91-GT-2.

Boyle, R. J., "Heat Transfer in Serpentine Passages With Turbulence Promoters," 1984, NASA TM 83614.

Chima, R. V., 1996, "A k-ω Turbulence Model for Quasi-Three-Dimensional Turbomachinery Flows," To appear at AIAA Aerospace Sciences Meeting. Also NASA TM 107051.

"GRIDPRO,™ /az3000, Users Guide and Reference Manual", 1993, Program Development Corporation, White Plains, NY.

"GRIDGEN, User's Manual for -," 1995, Pointwise, Inc.

Kays, W. M. and Crawford, M. E., 1980, "Convective Heat and Mass Transfer,", second Edition, MacGraw-Hill.

Liu, F. and Zheng, X., 1994, "A strongly-Coupled Time-Marching Method for Solving The Navier-Stokes and k-ω Turbulence Model Equations with Multigrid," AIAA-94-2389.

Menter, Florian R., 1993, "Zonal Two Equation k-ω Turbulence Models for Aerodynamic Flows," AIAA-93-2906.

Prakash, P and Zerkle, R., 1992, "Prediction of Turbulent Flow and Heat Transfer in a Radially Rotating Square Duct," *Journal of Turbomachinery*, Vol. 114, pp.835-846.

Snyder and Roelke, R. J., 1990, "Design of an Air-Cooled Metallic High Temperature Radial Turbine," *Journal of Propulsion and Power*, Vol. 6, pp. 283-288.

Schlichting, H., 1980, "Boundary-Layer Theory," Seventh Edition, McGraw-Hill Book Company.

Steinthorsson, E., Liou, M.-S., and Povinelli, L.A., 1993, "Development of an Explicit Multiblock/Multigrid Flow Solver for Viscous Flows in Complex Geometries," AIAA-93-2380.

Suo, M., 1978, "Turbine Cooling in the Aerothermodynamics of Aircraft Gas Turbines," AFAPL TR 78-52.

Taylor, J. R., 1980, "Heat Transfer Phenomena in Gas Turbines," ASME 80-GT-172.

Tekriwal, P., "Heat Transfer Predictions in Rotating Radial Smooth Channel: Comparative Study of k-ε Models with Wall Function and Low-Re Model," ASME paper 94-GT-196.

Wilcox, D. C., 1994a,"Turbulence Modeling for CFD," DCW Industries, Inc., La Canada, CA.

Wilcox, D. C., 1994b,"Simulation of Transition with a Two-Equation Turbulence Model," AIAA Journal, Vol. 32, No.2, pp. 247-255.

REPORT DOCUMENTATION PAGE

Public reporting burden for this collection of information is estimated to average 1 hour per response, including the time for reviewing instructions, searching existing data sources, gathering and maintaining the data needed, and completing and reviewing the collection of information. Send comments regarding this burden estimate or any other aspect of this collection of information, including suggestions for reducing this burden, to Washington Headquarters Services, Directorate for Information Operations and Reports, 1215 Jefferson Davis Highway, Suite 1204, Arlington, VA 22202-4302, and to the Office of Management and Budget, Paperwork Reduction Project (0704-0188), Washington, DC 20503.

1. AGENCY USE ONLY (Leave blank)	2. REPORT DATE October 1996	3. REPORT TYPE AND DATES COVERED Contractor Report

4. TITLE AND SUBTITLE

Internal Passage Heat Transfer Prediction Using Multiblock Grids and a k-ω Turbulence Model

6. AUTHOR(S)

David L. Rigby, Ali A. Ameri, and Erlendur Steinthorsson

5. FUNDING NUMBERS

WU–505–90–5K
NCC3–370

7. PERFORMING ORGANIZATION NAME(S) AND ADDRESS(ES)

Institute for Computational Mechanics in Propulsion
22800 Cedar Point Road
Cleveland, Ohio 44142

8. PERFORMING ORGANIZATION REPORT NUMBER

E–10489

9. SPONSORING/MONITORING AGENCY NAME(S) AND ADDRESS(ES)

National Aeronautics and Space Administration
Lewis Research Center
Cleveland, Ohio 44135–3191

10. SPONSORING/MONITORING AGENCY REPORT NUMBER

NASA CR–198540
ICOMP–96–8
96–GT–188

11. SUPPLEMENTARY NOTES

Prepared for the 41st Gas Turbine and Aeroengine Congress sponsored by the International Gas Turbine Institute of the American Society of Mechanical Engineers, Birmingham, United Kingdom, June 10–13, 1996. David L. Rigby, NYMA, Inc., 2001 Aerospace Parkway, Brook Park, Ohio 44142 (work funded under NASA Contract NAS3–27186); Ali A. Ameri, AYT Corporation, Brook Park, Ohio; and Erlendur Steinthorsson, Institute for Computational Mechanics in Propulsion, NASA Lewis Research Center (work funded under NASA Cooperative Agreement NCC3–370). ICOMP Program Director, Louis A. Povinelli, organization code 2600, (216) 433–5818.

12a. DISTRIBUTION/AVAILABILITY STATEMENT

Unclassified - Unlimited
Subject Category 34

This publication is available from the NASA Center for AeroSpace Information, (301) 621–0390.

12b. DISTRIBUTION CODE

13. ABSTRACT (Maximum 200 words)

Numerical simulations of the three-dimensional flow and heat transfer in a rectangular duct with a 180° bend were performed. Results are presented for Reynolds numbers of 17,000 and 37,000 and for aspect ratios of 0.5 and 1.0. A k-ω turbulence model with no reference to distance to a wall is used. Direct comparison between single block and multiblock grid calculations are made. Heat transfer and velocity distributions are compared to available literature with good agreement. The multi-block grid system is seen to produce more accurate results compared to a single-block grid with the same number of cells.

14. SUBJECT TERMS

Turbine cooling; Computational fluid dynamics; Heat transfer

15. NUMBER OF PAGES 12

16. PRICE CODE A03

17. SECURITY CLASSIFICATION OF REPORT	18. SECURITY CLASSIFICATION OF THIS PAGE	19. SECURITY CLASSIFICATION OF ABSTRACT	20. LIMITATION OF ABSTRACT
Unclassified	Unclassified	Unclassified	

NSN 7540-01-280-5500

Standard Form 298 (Rev. 2-89)
Prescribed by ANSI Std. Z39-18
298-102